The Role of Airmass Types and Surface Energy Fluxes in Snow Cover Ablation in the Central Appalachians

DANIEL J. LEATHERS

Center for Climatic Research, Department of Geography, University of Delaware, Newark, Delaware

DANIEL GRAYBEAL

Northeast Regional Climate Center, Cornell University, Ithaca, New York

THOMAS MOTE AND ANDREW GRUNDSTEIN

Department of Geography, University of Georgia, Athens, Georgia

DAVID ROBINSON

Department of Geography, Rutgers—The State University of New Jersey, New Brunswick, New Jersey

(Manuscript received 2 December 2003, in final form 11 June 2004)

ABSTRACT

A one-dimensional snowpack model, a unique airmass identification scheme, and surface weather observations are used to investigate large ablation events in the central Appalachian Mountains of North America. Data from cooperative observing stations are used to identify large ablation events within a 1° latitude × 1° longitude grid box that covers the majority of the Lycoming Creek basin in northern Pennsylvania. All 1-day ablation events greater than or equal to 7.6 cm (3 in.) are identified for the period of 1950 through 2001. Seventy-one events are identified, and these days are matched with a daily airmass type derived using the Spatial Synoptic Classification technique. Average meteorological characteristics on ablation days of each airmass type are calculated in an effort to understand the diverse meteorological influences that led to the large ablation events. A one-dimensional mass and energy balance snowpack model (''SNTHERM'') is used to calculate surface/atmosphere energy fluxes responsible for ablation under each airmass type. Results indicate that large ablation events take place under diverse airmass/synoptic conditions in the central Appalachians. Five airmass types account for the 71 large ablation events over the 52-yr period. Forty-three of the events occurred under ''moist'' airmass types and 28 under ''dry'' airmass conditions. Large ablation events under dry airmass types are driven primarily by daytime net radiation receipt, especially net solar radiation. These events tend to occur early and late in the snow cover season when solar radiation receipt is highest and are characterized by relatively clear skies, warm daytime temperatures, and low dewpoint temperatures. Moist airmass types are characterized by cloudy, windy conditions with higher dewpoint temperatures and often with liquid precipitation. During these events sensible heat flux is most often the dominant energy flux to the snowpack during ablation episodes. However, in many cases there is also a significant input of energy to the snowpack associated with condensation. Combinations of high sensible and latent heat fluxes often result in extreme ablation episodes, similar to those witnessed in this area in January 1996.

1. Introduction

Snow ablation is a major contributor to streamflow, soil moisture, and groundwater supplies in many areas of the world. As Ferguson and Morris (1987) point out, ''snowpacks are natural water reservoirs'' that, depending on the location, can release water to area streams at a consistent time from one year to the next. In such locations the consistent release of water to fill reservoirs, provide hydroelectric power, and replenish soil moisture supplies is a great benefit to a myriad of societal interests. In regions where snow cover is ephemeral, however, the lack of a single seasonal melt, or of consistency in volume or timing, has made forecasting the release of water from the snowpack a formidable challenge, leading to many harmful environmental and societal consequences. Snow cover ablation has been studied in many regions, including the Arctic and sub-Arctic (Ohmura 1981; Braithwaite and Olesen 1990; Rowe et al. 1995), many high-elevation mountain ranges (Marks

Corresponding author address: Dr. Daniel J. Leathers, Center for Climatic Research, Department of Geography, University of Delaware, 216 Pearson Hall, Newark, DE 19716-2541.
E-mail: leathers@udel.edu

© 2004 American Meteorological Society

and Dozier 1992; Pluss and Mazzoni 1994; McGregor and Gellatly 1996; Cline 1997), and in areas exhibiting ephemeral intraseasonal snow cover (Petzold 1981; Ferguson and Morris 1987; Grundstein and Leathers 1999). Interactions between the atmosphere and a melting snowpack have been explored in numerous studies. The consensus finding has been that the relative importance of individual energy balance components depends strongly on the geography of the region and the specific atmospheric conditions (e.g., Treidl 1970; Moore and Owens 1984; Kuusisto 1986; Robinson 1986; McGregor and Gellatly 1996; Hardy et al. 1998; Aizen et al. 2000; Koivusalo and Kokkonen 2002). In high-latitude and high-elevation regions, net radiation is usually identified as the most important energy input during snow cover ablation (Aguado 1985; Robinson 1986; Marks and Dozier 1992; Cline 1997; Hardy et al. 1998; Aizen et al. 2000; Koivusalo and Kokkonen 2002), while at lower latitudes and elevations, sensible and latent heat fluxes are often dominant (Treidl 1970; Moore and Owens 1984; Leathers et al. 1998; Grundstein and Leathers 1999).

The purpose of this study is to investigate the air–snow interface interactions during significant ablation events in a midlatitude area that experiences ephemeral seasonal snow cover. Specifically, a one-dimensional snowpack model, a unique airmass identification scheme, and surface weather observations will be used to investigate ablation events in the central Appalachian Mountains of North America.

2. Study area, data, and methodology

On 19 January 1996, the worst flooding on record occurred across a wide area of north-central Pennsylvania. This flooding was the result of the ablation of more than 0.5-m depth of snow cover and rainfall in excess of 7.5 cm (Leathers et al. 1998). The ablation occurred in less than 24 h and added more than 5.0 cm of additional water equivalent to the flooding streams. The Lycoming Creek basin (Fig. 1) was among the most adversely affected areas during this event, recording six fatalities, numerous injuries, and tens of millions of dollars lost in property damage. The meteorological and hydrological aspects of this event are detailed by Leathers et al. (1998), while Yarnal et al. (1997) describe the socioeconomic impacts. The basin is located in a transition region between the Ridge and Valley and Appalachians Plateau physiographic provinces in north-central Pennsylvania. It is covered by generally rugged terrain with interspersed areas of farmland and deciduous forest. Elevations within the basin range from approximately 150 m in the valleys to 700 m on the ridge tops. The basin has an area of approximately 700 km^2.

In order to identify large ablation events across the Lycoming basin, data from National Weather Service (NWS) cooperative observing stations were used. Specifically, the data from all stations residing in a 1° latitude × 1° longitude grid box centered on 41°N latitude and 77°W longitude were quality controlled using the routine developed by Robinson (1989). This routine flags suspect data based on a series of comparisons between snow-depth changes and daily temperature and precipitation statistics (Robinson 1989). These station data were used to calculate several diverse snow cover statistics for the grid cell, such as the mean snow depth, the median snow depth, the total number of stations, the time of observation of each station, and others. Data from between 8 and 15 stations were available for analysis within the grid box for each day from 1950 through 2001. For this study, the median snow depth in the grid cell was used to identify daily snow cover ablation events of 7.6 cm or greater. The 7.6-cm ablation criterion was chosen to select only those events with a significant water output from the snowpack, and yet allowed for a large enough number of cases for a meaningful analysis (71 cases). In addition, snow cover is measured by cooperative observers in English units in the United States, and the 7.6-cm criterion represents a change in depth of 3.0 in.

Clearly, decreases in snow depth are not always associated with melting of the snowpack. Settling of the pack can often lead to snow-depth decreases of several inches, especially following major snowfall events, and sublimation can lead to significant decreases in snow depth under favorable atmospheric conditions. In this study we have attempted to filter out all large ablation events that occur in direct association with significant snowfalls. The calculation of sublimation losses is beyond the scope of this study, and the reader is reminded that some of the snow-depth change that occurs may be the result of sublimation. It is also important to note that snow cover data from the cooperative network has no information on the water equivalent of the snowpack. Thus, the 7.6 cm (3.0 in.) ablation criterion does not reflect any specific output of water to the area streams. In fact, the water output to the streams may vary significantly, depending upon the density of the ablating snow.

Until recently, a major difficulty in examining relationships between snow cover ablation and airmass characteristics was the lack of information on air masses at a given location over a long time period. Kalkstein et al. (1998) and Sheridan (2002) have developed an automated routine to identify airmass types using hourly meteorological observations. The Spatial Synoptic Classification 2 (SSC2) uses discriminant analysis to each day identify a particular location as belonging to one of the following six airmass types: dry polar (DP), dry moderate (DM), dry tropical (DT), moist polar (MP), moist moderate (MM), and moist tropical (MT). There is also a transition (Tr) airmass category that represents a day on which an airmass transition occurred. Detailed general descriptions of these air masses are given in Sheridan (2002) and Leathers et al. (2002), while descriptions for the study area are given below. During the November through April snow cover season in northern Pennsylvania, only five

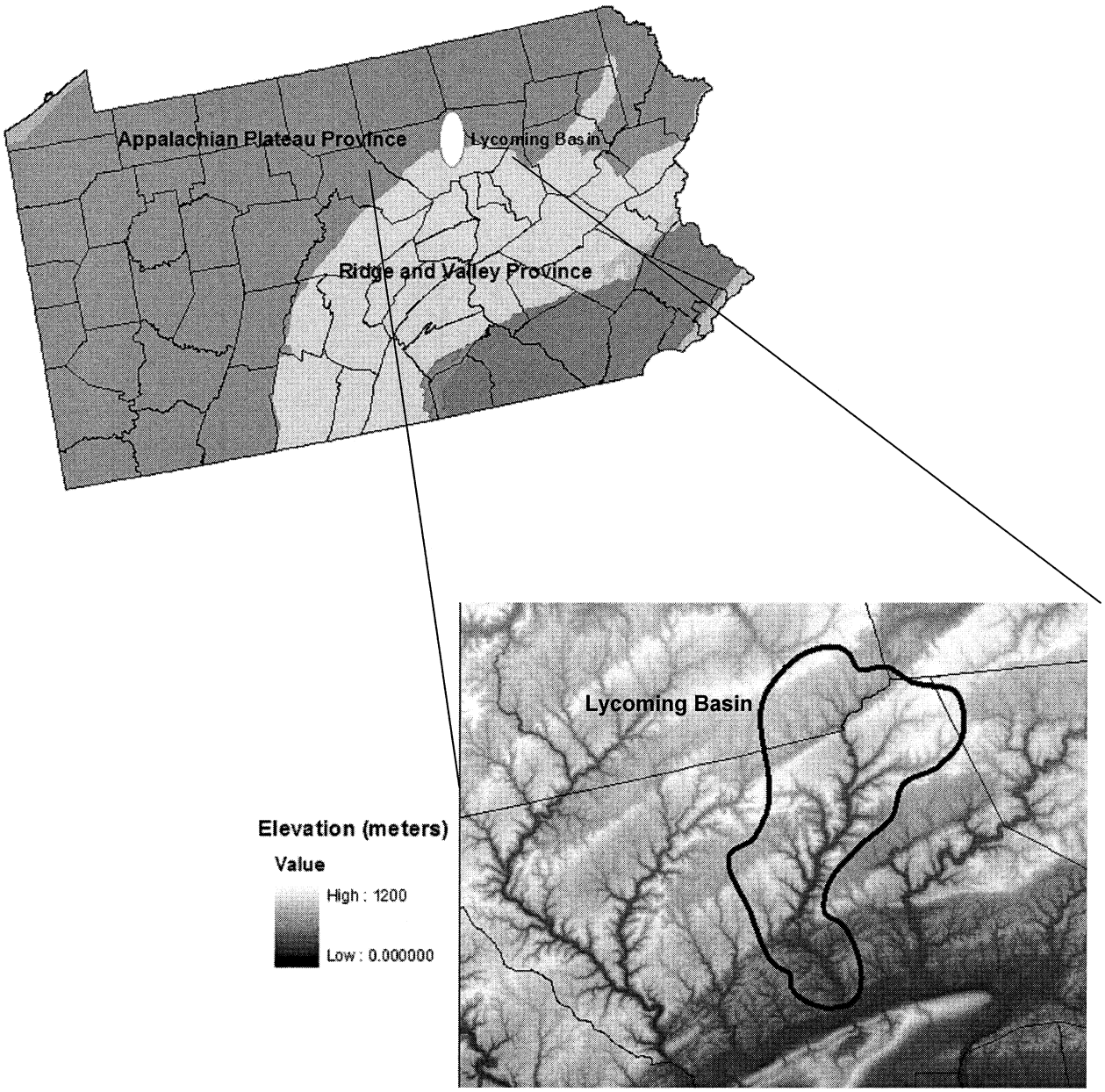

FIG. 1. Location of the Lycoming Creek basin.

of the seven types are commonly observed. Similar to classic continental polar (cP) air masses, DP types exhibit cold, dry atmospheric conditions originating in central Canada, while the DM type is characterized by a relatively warm, dry atmosphere similar to the ''Pacific'' air mass. Generally DM air is advected from the Pacific Ocean and warms adiabatically as it crosses the Rocky and Appalachian Mountains. The MP air masses represent the same conditions as maritime polar (mP) air masses in the classic system (cold, moist atmospheric conditions), typically originating over the North Atlantic Ocean, while the MM air masses are similar to MP, but warmer with higher dewpoint temperatures. Usually MM air masses are associated with an overrunning atmospheric situation ahead of the warm front of an advancing midlatitude cyclone. Transition days typically represent events when a front passes through the area causing diverse airmass conditions to occur on the same day. The airmass calendar for Williamsport, Pennsylvania (KIPT), the only NWS station residing in the $1° \times 1°$ grid cell (and the Lycoming Creek basin), is used to represent atmospheric conditions across the Lycoming Creek basin for the period of 1948 through 2001. SSC2 airmass types are spatially coherent over large regions, so that the air mass at KIPT corresponds to conditions across the entire highland, mid-Atlantic region. As an example, Table 1

TABLE 1. Characteristics of Jan airmass types for KIPT.

Airmass type	DM	DP	DT	MM	MP	MT	Tr
Frequency (%)	19.3	37.6	0.1	13.9	16.7	1.3	11.0
1600 LST temperature (°C)	4.0	−4.7	11.7	3.5	−1.4	11.9	−0.6
0400 LST temperature (°C)	−2.0	−11.0	−1.1	1.3	−4.2	4.4	−2.2
1600 LST dewpoint temperature (°C)	−5.6	−13.9	−8.3	0.0	−5.9	6.5	−7.8
Wind direction (avg)	270.0	270.0	180.0	90.0	270.0	120.0	270.0
Wind speed (m s^{-1}; avg)	3.7	4.1	5.4	3.4	3.5	3.4	5.4
Cloud cover (tenths)	6.2	5.0	1.8	9.5	9.1	9.5	7.7

gives the mean monthly characteristics of these airmass types for the midwinter month of January for KIPT that is located at 41.25°N, 76.92°W with an elevation of 159 m.

A one-dimensional mass and energy balance model (''SNTHERM,'' version 4; Jordan 1991) is used to calculate surface energy fluxes and snow cover ablation under the diverse airmass types. The model is designed for use with seasonal snow covers and can be used under common winter conditions, such as snowfall, rainfall, freeze–thaw cycles, and transitions between bare and snow-covered surfaces. Rather detailed meteorological observations are needed to drive the model, including temperature, dewpoint temperature, wind speed, cloud height, cloud type, cloud coverage, and precipitation. If available, solar radiation and longwave radiation values are also needed. If radiation flux data are not available (as in this study) the model calculates net solar flux based on cloud conditions (height and type), latitude, time of year and surface albedo, downwelling longwave radiation on the basis of air temperature, and upwelling longwave radiation from surface temperature and emissivity. Missing cloud-height data were estimated using a simple convective cloud-base scheme in which the surface dewpoint depression is multiplied by a constant value (Grundstein et al. 2002). Previous studies have indicated that the SNTHERM model gives reliable estimates for surface energy fluxes during snowpack ablation, and for the physical properties of the pack [depth, density, snow water equivalent (SWE), etc.; Rowe et al. 1995; Ellis and Leathers 1998; Grundstein et al. 2002]. Hourly meteorological data, for driving SNTHERM model runs, were obtained for the Williamsport NWS site from the National Climatic Data Center (NCDC) Surface Airways dataset.

Last, National Centers for Environmental Prediction (NCEP)–National Center for Atmospheric Research (NCAR) reanalysis data are used to define macroscale atmospheric circulation patterns associated with the diverse airmass types. Sea level pressure, and 500-hPa geopotential height data are used to create composite maps for each air mass. Compositing and mapping routines used in this study were from the National Oceanic and Atmospheric Administration (NOAA)–Cooperative Institute for Research in Environmental Sciences (CIRES) Daily Mean Compositing Web page (available online at http://www.cdc.noaa.gov/Composites/Day/).

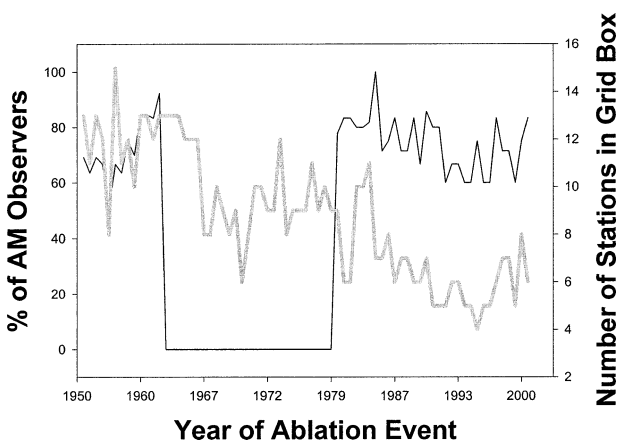

FIG. 2. Percentage of A.M. observers within the grid box (thin dark line) and the number of stations within the box (thick gray line) over the period of record.

3. Results

Substantial ablation days (at least 7.6 cm) were identified for the Lycoming Creek basin area by calculating the difference between the median snow cover on successive days for stations residing in the 1° latitude × 1° longitude grid box. To determine the day on which the ablation event occurred, it was important to know the time of observation of the stations within the grid box. When the majority of the stations were morning (A.M.) observers, the air mass on the day at the beginning of the differenced pair was used to represent conditions during the ablation event. When the majority of the stations were afternoon (P.M.) observers, the day at the end of the differenced pair was used. Figure 2 shows the percentage of A.M. observers within the grid cell and the number of stations within the cell over the period of record. It is clear that A.M. observers are most prevalent except for the period of 1964 through 1981, when all observers are listed as P.M. The listing of observation time as P.M. for all stations during this period is believed to be an error inherent in the NCDC metadata. Therefore, during this period the decision to use the first or second day of the differenced pair was made by inspection of the meteorological situation. It is also clear from Fig. 2 that the total number of stations in the grid cell decreased consistently through the period of record

TABLE 2. Dates of days with at least 7.6-cm ablation based on the median value in the grid box covering the Lycoming Creek basin. Boldface dates are those used in the subsequent modeling analysis.

Year	Month	Day	Airmass type
1953	**Nov**	**9**	**DM**
1963	**Feb**	**20**	**DM**
1964	**Jan**	**21**	**DM**
1966	Feb	12	DM
1966	Feb	14	DM
1966	Feb	26	DM
1967	Mar	10	DM
1967	Nov	19	DM
1971	Jan	5	DM
1971	Mar	6	DM
1976	Jan	14	DM
1978	**Mar**	**19**	**DM**
1979	**Feb**	**22**	**DM**
1987	**Feb**	**2**	**DM**
1994	**Mar**	**23**	**DM**
1998	**Jan**	**2**	**DM**
2000	**Feb**	**10**	**DM**
1959	Mar	14	DP
1977	**Mar**	**20**	**DP**
1982	**Apr**	**8**	**DP**
1982	**Apr**	**10**	**DP**
1984	**Mar**	**15**	**DP**
1984	**Mar**	**31**	**DP**
1987	**Jan**	**4**	**DP**
1993	**Mar**	**16**	**DP**
1993	**Mar**	**21**	**DP**
1993	**Mar**	**22**	**DP**
1994	**Mar**	**19**	**DP**
1951	**Dec**	**21**	**MM**
1951	**Dec**	**31**	**MM**
1961	Feb	14	MM
1966	Feb	11	MM
1967	Mar	11	MM
1968	Nov	15	MM
1971	Feb	19	MM
1972	Mar	16	MM
1977	**Feb**	**13**	**MM**
1982	**Mar**	**11**	**MM**
1985	**Feb**	**12**	**MM**
1990	**Dec**	**29**	**MM**
1990	**Dec**	**30**	**MM**
1992	**Feb**	**14**	**MM**
1992	**Dec**	**11**	**MM**
1994	**Mar**	**7**	**MM**
1996	**Jan**	**17**	**MM**
1996	**Jan**	**18**	**MM**
1950	**Mar**	**23**	**MP**
1953	**Nov**	**8**	**MP**
1955	Dec	24	MP
1958	Mar	14	MP
1960	**Mar**	**17**	**MP**
1961	Apr	10	MP
1968	Nov	14	MP
1970	Mar	31	MP
1970	Apr	1	MP
1972	Dec	2	MP
1983	**Apr**	**20**	**MP**
1984	**Mar**	**30**	**MP**
1987	**Jan**	**11**	**MP**
1987	**Nov**	**12**	**MP**
1994	**Mar**	**3**	**MP**
1994	**Mar**	**21**	**MP**
1996	**Jan**	**13**	**MP**

TABLE 2. (*Continued*)

Year	Month	Day	Airmass type
1959	Mar	15	Tr
1964	Jan	25	Tr
1972	Feb	21	Tr
1973	Dec	21	Tr
1976	Mar	11	Tr
1978	Jan	26	Tr
1981	**Feb**	**11**	**Tr**
1996	**Jan**	**15**	**Tr**

from as high as 14 stations in the 1950s to around 6 at the end of the record. Seventy-one days during the period of 1950 through 2001 were identified as experiencing ablations of 7.6 cm or greater (Table 2). These ablation days were subsequently matched with airmass types from the airmass calendar for Williamsport.

a. Meteorological conditions during ablation events

Table 3 shows the basic meteorological conditions on large ablation days represented by data from the Williamsport NWS site. Seventeen of the large ablation days occurred under a DM air mass. These days had one of the smallest average snowpack ablations (9.6 cm) and were characterized by the highest afternoon temperatures (8.9°C), a relatively dry atmosphere, partly cloudy conditions, and low wind speeds. On 11 of the large ablation days DP air masses were in place. During these days skies were partly cloudy, daytime temperatures were moderately warm (6.6°C), dewpoint temperatures were the lowest of all of the airmass types, and wind speeds were moderate. Overrunning conditions associated with MM airmass types were present on 18 of the large ablation days, the largest number of days in any category. These days had the largest 24-h ablation totals (11.4 cm), dewpoint temperatures above 0°C, and average liquid precipitation of 0.38 cm, with precipitation falling on each of the 18 days. The MP air masses were also associated with a large number of ablation days (17 days). Moist polar airmass types were characterized by significant snowpack ablation, the coldest daytime temperatures (4.1°C), a relatively moist atmosphere, and significant liquid precipitation totals (0.78 cm), with precipitation on 94% of the days. Last, large ablation events occurred on eight Tr airmass days. These days had moderate ablation totals (10.3 cm), a large diurnal range in temperature, relatively high wind speeds, and the greatest values of liquid precipitation (1.55 cm). Rainfall occurred on all but one of the transition days.

NCEP–NCAR reanalysis data were used to create composites of atmospheric conditions under each of the airmass types during days of 7.6 cm or greater ablation. Figures 3–7 show the sea level pressure and 500-hPa-height patterns for each air mass. Note that surface wind observations at the Williamsport NWS station are often

TABLE 3. Meteorological conditions on large ablation days represented by data from KIPT.

Airmass type	No. days	Ablation (cm)	High (°C)	Low (°C)	Avg temperature (°C)	Avg dewpoint (°C)	RH (%)	Avg cloud cover (tenths)	SLP (hPa)	Wind direction (°)	Wind speed (m s^{-1})	Liquid precipitation (cm)	Snow (cm)
DM	17	9.6	8.9	−2.8	3.1	−3.6	65	6.2	1014	SSE 170	3.6	0.03	0.00
DP	11	9.6	6.6	−5.4	0.6	−6.6	61	5.9	1021	SW 202	4.1	0.05	0.65
MM	18	11.4	6.8	0.1	3.5	0.2	83	9.1	1015	SE 127	4.1	0.38	0.43
MP	17	10.7	4.1	−2.0	1.1	−2.3	78	9.1	1008	SW 211	4.7	0.78	3.63
Tr	8	10.3	7.5	−6.8	0.4	−3.0	72	8.1	1007	SW 192	6.1	1.55	1.6

affected by local topography and may not be consistent with the large-scale winds resulting from the synoptic situation. Dry, moderate ablation days across the Lycoming Creek basin are characterized by an area of low pressure over the Maritime Provinces of Canada and an area of high pressure centered in the area of Bermuda (Fig. 3a). This configuration leads to surface westerly and southwesterly flow across the basin, advecting relatively warm, dry air over the region from the western side of the high pressure area. At 500 hPa, the flow is primarily zonal across much of the eastern United States during these events (Fig. 3b). The majority of these events occur during February and March (Table 2), explaining the relatively high daytime temperatures.

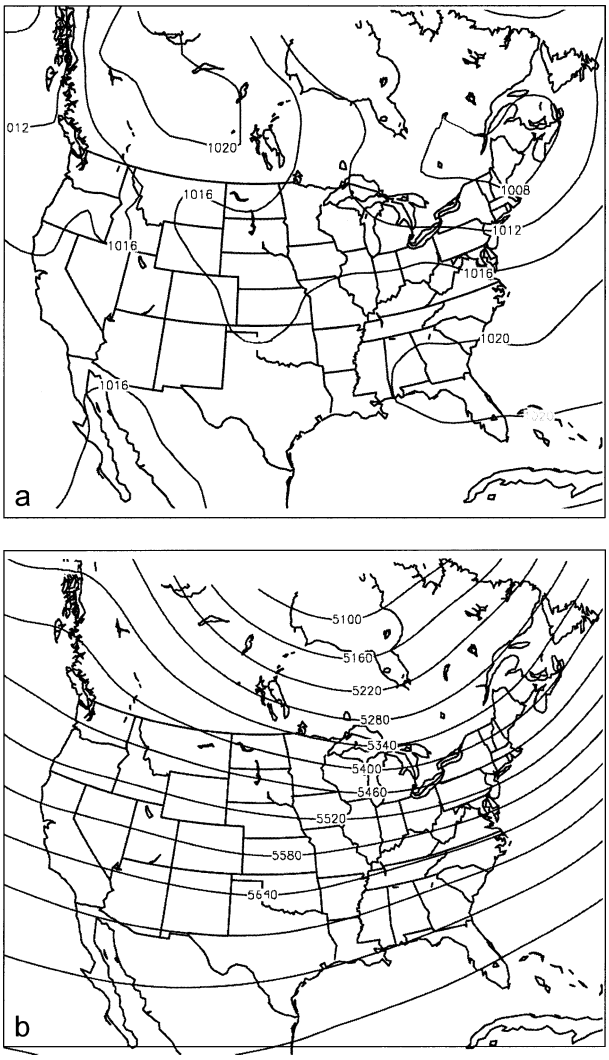

FIG. 3. Composite values of (a) sea level pressure (hPa), and (b) 500-hPa geopotential heights (gpm) for DM airmass type.

An area of high pressure centered over the eastern United States and low pressure exiting eastern Canada (Fig. 4a) characterize the synoptic conditions on DP airmass days. Surface winds are generally from the west across the basin (Fig. 4a), while a trough is exiting the region at the 500-hPa level (Fig. 4b). This synoptic pattern brings cool, dry air across the region, along with generally partly cloudy conditions. It is notable that 10 of the 11 DP ablation days occurred during either March or April, explaining the relatively warm temperatures even under an air mass that originates in central Canada.

Strong high pressure over the Atlantic combines with an area of low pressure moving through the upper Mississippi River valley (Fig. 5a) to generate the conditions observed on MM airmass days. Surface winds with a southerly or southeasterly component dominate on these days, bringing relatively warm, moist air over the basin. This airmass type is usually associated with the movement of a warm front through the mid-Atlantic region. At 500 hPa winds are from the southwest, in response to the movement of a broad trough through the northern plains (Fig. 5b). Overrunning precipitation often occurs with this synoptic pattern, further enhancing the snowpack ablation. An inspection of Table 2 shows that this synoptic situation can lead to large ablations at any time during the snow cover season.

A distinct area of low pressure off the southern New England coast is characteristic of MP airmass ablation days (Fig. 6a). In this case, northerly winds, in association with the low pressure area, bring maritime polar air from the Atlantic over the Lycoming basin either directly, or as a ''wraparound'' once the storm has passed to the north. A 500-hPa trough is located across the northeast United States during these events, supporting the development of the coastal low (Fig. 6b). High relative humidities, cloud cover, and precipitation often accompany this airmass situation. In fact, snowfall often occurs across northern Pennsylvania as the low

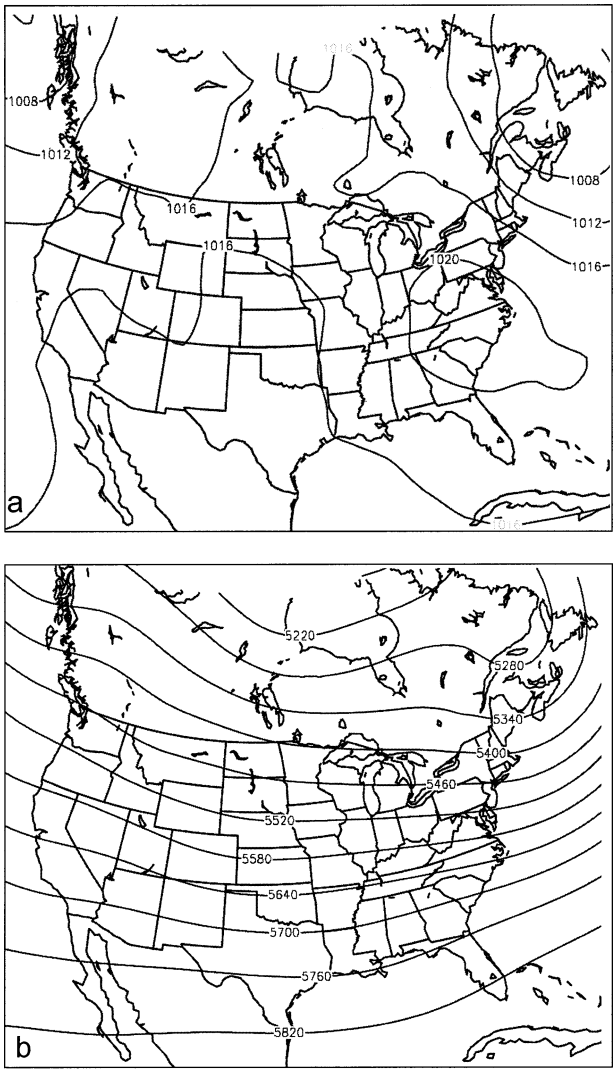

FIG. 4. Same as Fig. 3, but for DP airmass type.

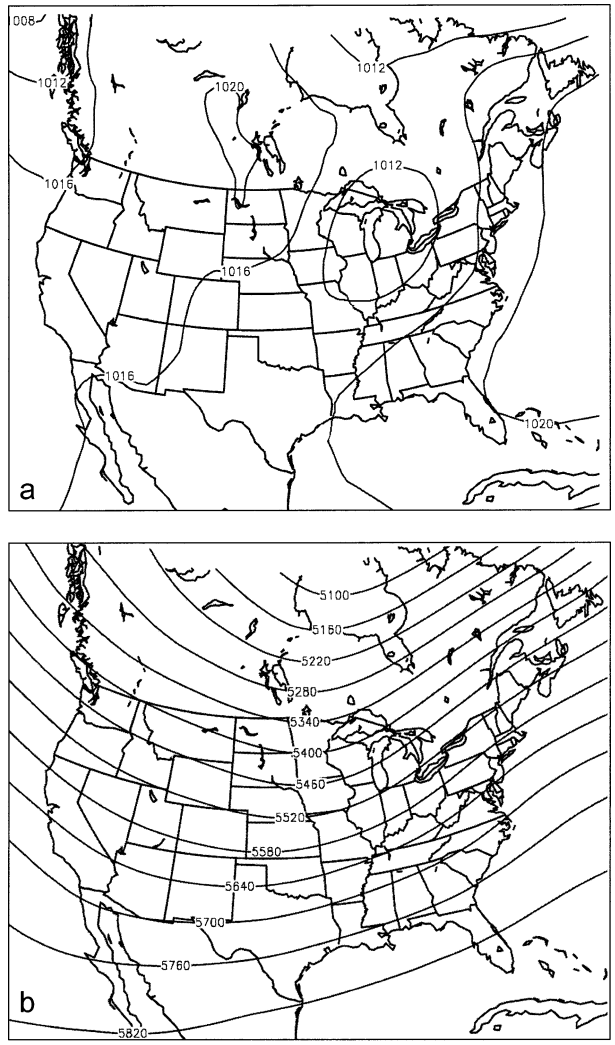

FIG. 5. Same as Fig. 3, but for MM airmass type.

pulls away to the north, restoring some of the ablated pack.

Transition airmass days are associated with a strong area of low pressure moving through the St. Lawrence River valley, west of the Lycoming basin (Fig. 7a). This puts the basin in the warm sector of the storm, with winds possessing a strong southerly component evident across the region. A strong 500-hPa trough is apparent in the composites across the upper Midwest, supporting the surface low (Fig. 7b). As this synoptic type progresses, an approaching cold front often leads to significant liquid precipitation across the mid-Atlantic, which enhances the ablation rate. Cold-air advection behind the front often causes freezing of the remaining snow cover, and a rapid end to the ablation event.

b. Airmass specific surface energy fluxes

The energy budget equation for a snowpack is given as

$$Q_{\text{net}} = \text{Kn} + \text{Ln} + H + \text{LE} + G + \text{Qp}, \qquad (1)$$

where Q_{net} is the net energy available to the snowpack, Kn is the net shortwave flux, Ln is the net longwave flux, H is sensible heat flux, LE is latent heat flux, G is ground heat flux, and Qp is the flux of energy from precipitation.

The SNTHERM snowpack model was used to derive modeled values for surface energy fluxes under the five airmass types. Hourly meteorological data from KIPT were used to drive the model. Unfortunately, the KIPT station, like many others, has not had consistent observing, reporting, and digitizing practices over the last half century. In some years, data were digitized only on a 3-hourly basis. In other years, the station was closed for at least a portion of each day, usually during the nighttime hours. Therefore, SNTHERM could not be run for all days within each airmass type. Those dates highlighted in Table 2 indicate the availability of hourly

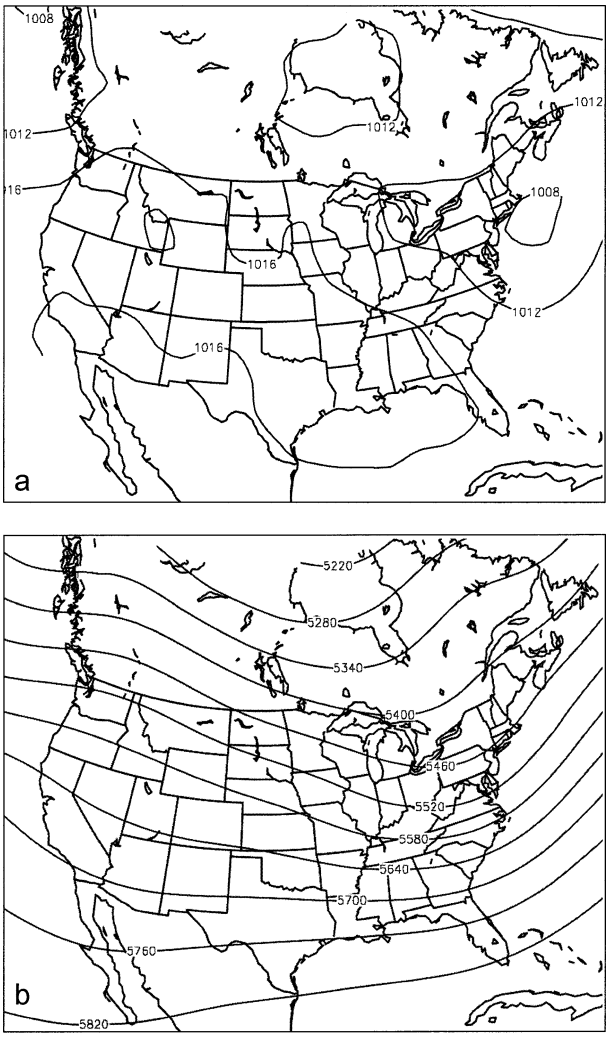

FIG. 6. Same as Fig. 3, but for MP airmass type.

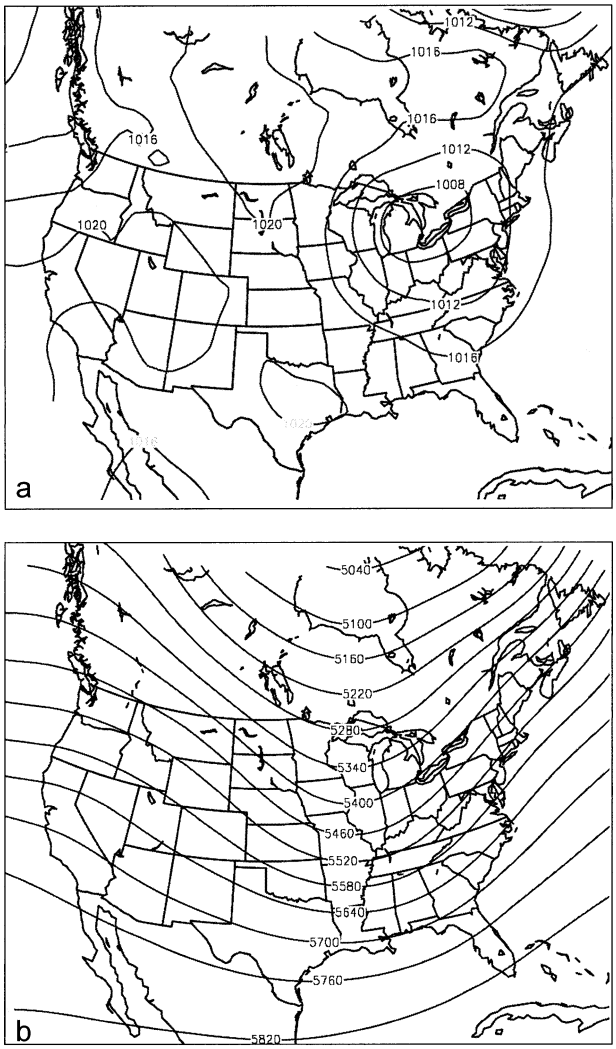

FIG. 7. Same as Fig. 3, but for Tr airmass type.

data and their use as part of the modeled energy flux ensemble for each airmass type.

The model was initialized with a beginning snow depth of 1.4 m for each case. This depth was chosen to ensure that the snowpack did not melt over the 2-day spin-up period and the day being modeled (3-day model run). The albedo of the pack was originally set at 0.8; however, a variable albedo routine within the model modifies this value according to the pack parameters, such as grain size, density, and so on. As mentioned above, a 2-day ''spinup'' time (the two previous calendar days) was used to bring the model to equilibrium before modeling the day of interest. Hourly surface energy flux values were derived for each day of a given airmass type. The hourly values for each day were averaged to derive the modeled ensemble value for each airmass type. Table 4 shows the modeled ensemble flux components for each type, while Figs. 8a–8e show box plots for each flux component. Note that positive flux values indicate energy toward the surface (into the snowpack), while negative values indicate fluxes away from the surface.

Nine of the 17 ablation days with a DM airmass type had hourly meteorological data available for modeling. Figure 8a shows that dry, moderate days are characterized by relatively large net solar radiation values, negative net longwave radiation values, and smaller positive values of sensible heat flux, and negative values of latent heat flux. During daylight hours, net radiation values were positive and into the snowpack, while net radiation values averaged over the entire day were near zero (negative net radiation values at night). For DM airmass types the major contributor to melt was the input of solar radiation to the pack during daylight hours. Sensible heat flux was also a significant contributor to the energy available for ablation, but was smaller than the magnitude of solar radiation (Table 4). Latent heat and ground heat fluxes were uniformly small during this weather situation.

TABLE 4. Average modeled flux components for each airmass type during large ablation days. Flux values are in watts per square meter (Kd is downward shortwave radiation, Ld is downward longwave radiation, Lu is upward longwave radiation, and Net is net radiation), *T* is mean temperature (°C), RH is relative humidity (%), and Ws is wind speed (m s^{-1}).

Type	Kn	Kd	Ln	Ld	Lu	*H*	LE	*G*	*T*	RH	Ws	Net
DM	93.3	436.3	−35.9	265.3	302.6	58.6	−19.4	0.3	3.2	64.3	3.3	−0.6
DP	124.0	584.4	−42.7	252.4	296.7	54.5	−37.0	0.3	0.7	60.9	4.2	6.7
MM	37.5	285.5	−7.4	304.8	312.8	53.3	2.4	0.4	2.8	83.4	4.2	6.8
MP	45.3	379.7	−13.9	294.4	308.7	56.9	−21.0	0.2	1.1	76.3	5.3	4.7
Tr	108.7	510.4	−39.3	258.9	299.6	56.5	−28.2	0.3	1.9	62.6	3.7	3.0
Avg	81.8	439.3	−27.8	275.1	304.1	56.0	−20.6	0.3	2.0	69.5	4.1	4.1

Of the 11 DP ablation days, 10 had sufficient hourly data for modeling. The clear skies associated with the DP airmass type, and the tendency to occur during March and April, resulted in the highest values of solar radiation receipt (Kn) of all the airmass patterns (Fig. 8b; Table 4). Net radiation values were large and positive during the daylight hours, and relatively large and negative at night, resulting in a 24-h value near zero. Although *H* values were significant, they were generally offset by negative LE fluxes of nearly the same magnitude. The strong negative LE fluxes indicate large evaporation rates as the snow melts and the resulting water evaporates readily into the dry atmosphere. This evaporation acts to cool the pack and slow ablation processes. Similar to the DM airmass type, Kn was the major contributor to melt under these airmass conditions, with values more than twice that of the *H* fluxes.

Eighteen of the large ablation events occurred on days with the MM airmass type, and hourly data were available on 12 of these days. During MM days, the cloud

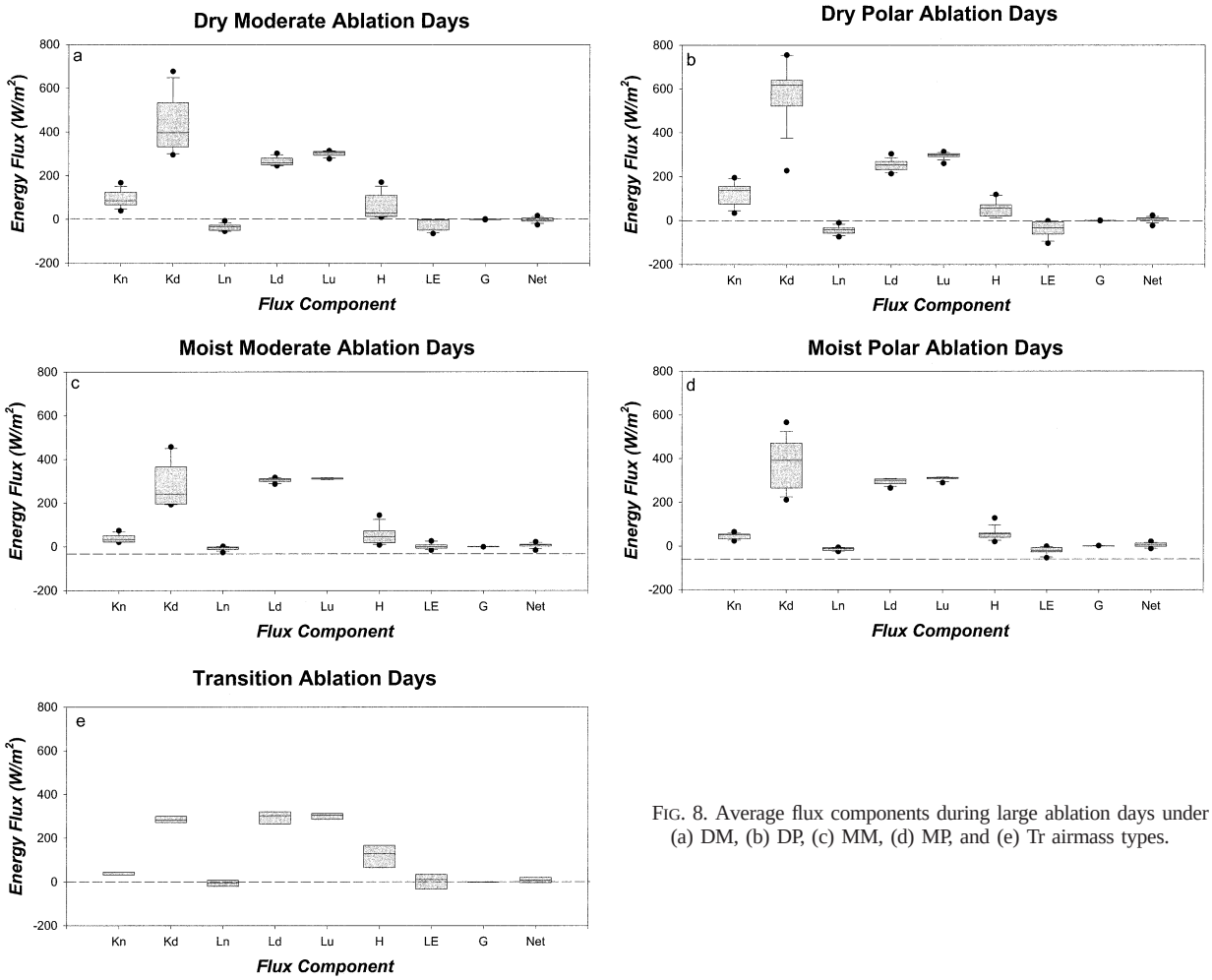

FIG. 8. Average flux components during large ablation days under (a) DM, (b) DP, (c) MM, (d) MP, and (e) Tr airmass types.

cover associated with the overrunning situation limited Kn values significantly (Fig. 8c; Table 4). Thus, little solar radiation was available for melt on these days. Instead, relatively high temperatures and dewpoint temperatures, in conjunction with breezy conditions, resulted in significant positive values of both *H* and LE fluxes, both of which contributed to ablation. Although the average LE flux during these situations was not large (2.4 W m^{-2}), individual hourly values were often equivalent to the *H* values. These large positive LE fluxes are a result of condensation of atmospheric moisture onto the snowpack when dewpoint temperatures rise above 0°C. On MM days, *H* fluxes are the largest overall contributor to ablation, with net radiation values of nearly the same magnitude during the daylight hours. In addition, liquid precipitation during these events undoubtedly enhances ablation processes.

The MP airmass type occurred on 17 of the large ablation days. Unfortunately, only 10 of the MP days had the hourly data needed for use in the SNTHERM model. Because of the extensive cloud cover associated with this airmass type, Kn values are relatively small during these events, but as Fig. 8d shows, the day-to-day variability is large (see Kd values). Similar to MM days, *H* fluxes provide the largest input of energy to the melting pack (Table 4), at least when averaged over the entire day. Under MP conditions, dewpoint temperatures are lower (Table 3), and there is little condensation on to the pack. In fact, LE fluxes are generally directed away from the pack as evaporation of the melted water takes place, acting to cool the pack and inhibit ablation. Thus, daylong *H* fluxes along with the daytime input of solar radiation lead to large ablation under MP conditions, along with input of energy from liquid precipitation.

Unfortunately, only two of the eight ablation days associated with Tr airmass situations had the data needed for modeling. However, these days are generally associated with relatively extensive cloud cover, large temperature ranges, and significant liquid precipitation (Table 3). The model results for the two runs indicate that these days are much like both MM and MP events, with *H* and Kn fluxes providing the majority of the energy for snow ablation (Fig. 8e). A major difference with these events is that a period of strong ablation is usually followed by cold and windy conditions as a cold front passes through the area, quickly ending any ablation processes. Because the frontal passage occurs sometime during the 24-h period, thus, limiting the melt to less than 24 h, these events often include short, intense ablation periods (Leathers et al. 1998). An inspection of the individual cases indicates that positive LE fluxes are often of great importance in these situations as very moist air is advected into the area ahead of the approaching cold front. These LE fluxes can have magnitudes of greater than 300 W m^{-2} in some instances.

In general, ablation processes within the Lycoming basin are dependent upon the nature of the synoptic weather type affecting the area. Figure 9 shows mean daily energy flux values for the major flux components under the diverse airmass types. During types with dry atmospheric conditions (DM, DP), the major contributor to melt is daytime net radiation (represented by Kn). Daytime Kn values are generally 2–3 times the magnitude of any other energy flux under these airmass conditions. Ablation under moist airmass types is primarily driven by sensible and, in some cases, latent heat fluxes. Mean daily sensible heat flux values (*H*) are the largest fluxes for MM and MP airmass types (Fig. 9). Although mean values of latent heat flux are near zero for the moist types, in some cases the flux of latent heat can be very important in the ablation process. Two case studies will be presented that illustrate typical conditions under these general airmass types.

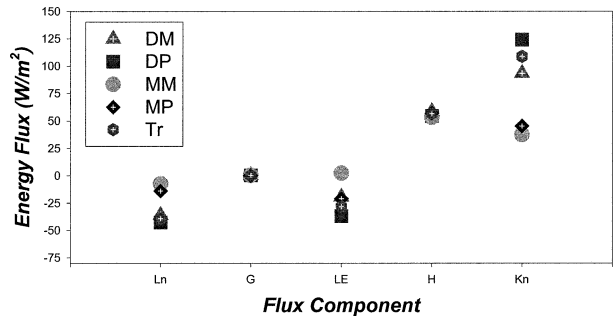

FIG. 9. Mean daily energy flux values for the major flux components under the diverse airmass types.

c. Case studies

Two case studies will be used to illustrate the general conditions during ablation events under both a dry and moist airmass type. Figure 10a shows modeled snow depth, net radiation, and sensible heat fluxes for 15 March 1984, a day identified as being a DP (dry) type. Observed snow depth decreased by 7.6 cm over the 24-h period (median across the 1° latitude × 1° longitude box), while modeled depth changes were 9.2 cm. It is clear from Fig. 10a that the majority of melt took place during the period between about 1000 and 1500 LST, matching very closely the time with maximum net radiation values. Until about 0800 LST, net radiation values are negative, implying a cooling of the pack from radiative processes. Values become positive after this time and remain so until midafternoon, being dominated by solar radiation fluxes. Sensible heat flux values throughout the 24-h period are uniformly small and positive, never reaching values above 20 W m^{-2}, an order of magnitude smaller than the midday net radiation values. Thus, the dominant energy flux associated with melt on this day was clearly midday net radiation, and the majority of the melting took place during the midday hours. This day is very similar to others of the DM or DP airmass types.

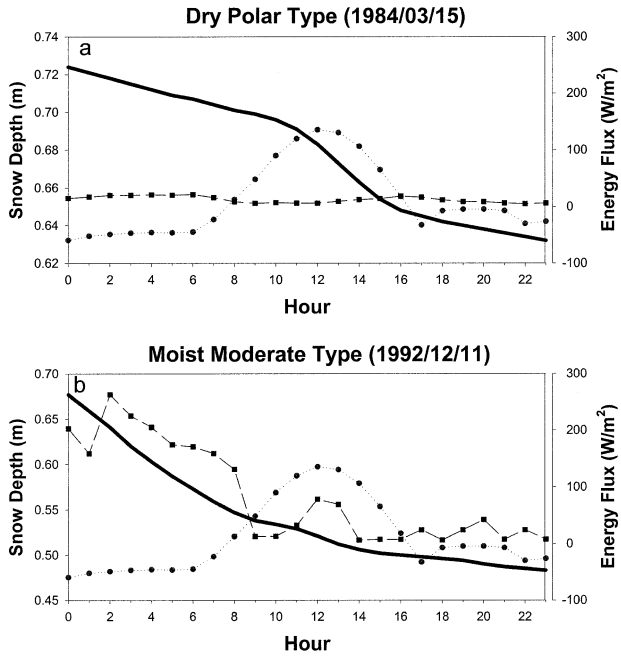

FIG. 10. Snow depth (solid line), net radiation (dashed line with circles), and sensible heat flux (long dashes with squares) during selected ablation events under both (a) dry and (b) moist airmass types.

Ablation processes are very different under the moist airmass types. Figure 10b shows conditions on 11 December 1992, a day classified as MM (a moist type). Observed snow depth decreases in the 1° latitude × 1° longitude box were approximately 13 cm over the 24-h period, while modeled depth changes were larger (nearly 19 cm). Observed median snow cover values decreased to zero by the end of the period, limiting the amount of melt that could have occurred under these atmospheric conditions. The amount of snow available for melt was not limited in any way in the model because of the large layer of snow present at the beginning of the model spinup process. On this day, the most intense period of melt occurs between 0000 and 0800 LST. During this period, nearly 13 cm of melt takes place. Net radiation values during this intense ablation period are significantly negative, indicating a cooling of the snowpack. However, sensible heat flux values are large and positive at this time, reaching values over 200 W m^{-2} in the predawn hours. After 0800 LST, sensible heat flux values decrease substantially to less than 50 W m^{-2} while net radiation values increase to approximately 100 W m^{-2} during midday hours. Although ablation continues throughout the day, it continues at a reduced rate compared to the period with large sensible heat flux. It is clear that sensible heat flux dominated the melt processes during this period, because the majority of the melt occurred with negative net radiation values. This day is similar to the majority of MM and MP airmass types where positive sensible and, in some cases, latent heat fluxes are responsible for the majority of the ablation. It should be noted that even on these days, net radiation is also an important contributor to melt during the midday hours. The ablation event of January 1996, discussed in the introduction, was similar to this case study, except that much of the ablation in that case was associated with latent heat release due to condensation on to the snowpack.

4. Summary and conclusions

A one-dimensional snowpack model, a unique airmass identification scheme, and surface weather observations were used to investigate large (>7.6 cm) ablation events in the central Appalachian Mountains of North America. Specifically, the Lycoming Creek basin of north-central Pennsylvania was chosen for study because of its history of severe flooding events over the last century. Data from cooperative observing stations were used to identify large ablation events within a 1° latitude × 1° longitude grid box that covered the majority of the Lycoming Creek basin. All 1-day ablation events greater than or equal to 7.6 cm were identified for the period of 1950 through 2001. Seventy-one events were identified, and these days were matched up with a daily airmass weather type, derived using the Spatial Synoptic Classification technique (Kalkstein et al. 1998; Sheridan 2002). Average meteorological characteristics on ablation days of each airmass type were calculated in an effort to understand the diverse meteorological influences that led to the large ablation events. Subsequently, a one-dimensional mass and energy balance snowpack model (SNTHERM; Jordan 1991) was used to calculate surface/atmosphere energy fluxes responsible for ablation under each airmass type. The major findings of this work include the following:

1) Large ablation events take place under diverse airmass/synoptic conditions in the central Appalachians. Five airmass types account for the 71 large ablation events over the 52-yr period. Forty-three of the events occurred under ''moist'' airmass types, including moist moderate (MM), moist polar (MP), and transition (Tr) days. Large ablations associated with moist airmass types occur throughout the snow cover season (November–April). Dry moderate (DM) and dry polar (DP) types account for the other 28 large ablation events. Most DM- and DP-driven ablation days occur either early, or most frequently late in the snow cover season.
2) Large ablation events under dry airmass types (DM and DP) are driven primarily by daytime net radiation receipt, especially net solar radiation. These events tend to occur early and late in the snow cover season when solar radiation receipt is at its highest. These days are characterized by relatively clear skies, warm daytime temperatures, and low dewpoint temperatures.
3) Moist airmass types are characterized by cloudy,

windy conditions with higher dewpoint temperatures and, often, with liquid precipitation. During these events sensible heat flux is most often the dominant energy flux to the pack during ablation episodes. However, in many cases there is also a significant input of energy to the pack associated with condensation. As air with dewpoint temperatures in excess of 0°C moves over the pack, condensation occurs on the pack, releasing large amounts of energy during the phase transition. Combinations of high sensible and latent heat fluxes often result in extreme ablation episodes, similar to that witnessed in this area in January 1996 (Leathers et al. 1998).

Thus, it is clear that in ephemeral snow cover regions, diverse airmass conditions lead to large ablation events, and that each airmass condition produces its own set of surface energy fluxes responsible for snowpack ablation. This same methodology is currently being used to examine ablation across the northern Great Plains of the United States, in a climatic region that is very different from that found across the central Appalachians. This study did not address the influence of snowpack characteristics on the ablation process (age, grain size, temperature profile, etc.). The authors are currently using the snowpack model used in this study (SNTHERM) to investigate the pack morphology and dynamics during ablation events of different character. It is hoped that continued research on the interactions between the atmosphere and ablating snowpacks will lead to a reduction in fatalities, injuries, and property damage associated with snow ablation–induced flooding.

Acknowledgments. This research was supported by Grant NAG5-11452 from the National Aeronautics and Space Administration. The authors thank Drs. Scott Sheridan and Lawrence Kalkstein for use of the spatial synoptic classification.

REFERENCES

Aguado, E., 1985: Radiation balances of melting snow covers at an open site in the central Sierra-Nevada California. *Water Resour. Res.,* **21,** 1649–1654.

Aizen, E. M., E. B. Aizen, J. M. Melack, and A. N. Krenke, 2000: Heat exchange during snow ablation in plains and mountains of Eurasia. *J. Geophys. Res.,* **105** (D22), 27 013–27 022.

Braithwaite, R. J., and O. B. Olesen, 1990: A simple energy balance model to calculate ice ablation at the margin of the Greenland ice sheet. *J. Glaciol.,* **36,** 222–228.

Cline, D. W., 1997: Snow surface energy exchanges and snowmelt at a continental, midlatitude Alpine site. *Water Resour. Res.,* **33,** 689–701.

Ellis, A. W., and D. J. Leathers, 1998: The effects of a discontinuous snow cover on lower atmospheric temperature and energy flux patterns. *Geophys. Res. Lett.,* **25,** 2161–2164.

Ferguson, R. I., and E. M. Morris, 1987: Snowmelt modeling in the Cairngorms, NE Scotland. *Trans. Roy. Soc. Edinburgh: Earth Sci.,* **78,** 261–287.

Grundstein, A. J., and D. J. Leathers, 1999: A spatial analysis of snow-surface energy exchanges over the northern Great Plains of the United States in relation to synoptic scale forcing mechanisms. *Int. J. Climatol.* **19,** 489–511.

——, T. Mote, and D. Leathers, 2002: A hybrid climatology of snow water equivalent over the northern Great Plains of the United States. *Polar Geogr.,* **26,** 187–209.

Hardy, J. P., R. E. Davis, R. Jordan, W. Ni, and C. E. Woodcock, 1998: Snow ablation modeling in a mature aspen stand of the boreal forest. *Hydrol. Process.,* **12,** 1763–1778.

Jordan, R., 1991: A one dimensional temperature model for snow cover: Technical documentation for SNTHERM.89. U.S. Army Corps of Engineers, Cold Regions Research and Engineering Laboratory Special Rep. 91-16, 49 pp.

Kalkstein, L. S., S. C. Sheridan, and D. Y. Graybeal, 1998: A determination of character and frequency changes in air masses using a spatial synoptic classification. *Int. J. Climatol.,* **18,** 1223–1236.

Koivusalo, H., and T. Kokkonen, 2002: Snow processes in a forest clearing and in a coniferous forest. *J. Hydrol.,* **262,** 145–164.

Kuusisto, E., 1986: The energy balance of a melting snow cover in different environment. Modeling Snowmelt-Induced Processes, IAHS Publication 155, 37–45.

Leathers, D. J., D. R. Kluck, and S. Kroczynski, 1998: The severe flooding event of 1996 across north-central Pennsylvania. *Bull. Amer. Meteor. Soc.,* **79,** 785–797.

——, T. L. Mote, A. J. Grundstein, D. A. Robinson, K. Felter, K. Conrad, and L. Sedywitz, 2002: Associations between continental-scale snow cover anomalies and air mass frequencies across eastern North America. *Int. J. Climatol.,* **22,** 1473–1494.

Marks, D., and J. Dozier, 1992: Climate and energy exchange at the snow surface in the alpine region of the Sierra Nevada, 2, snow cover energy balance. *Water Resour. Res.,* **28,** 3043–3054.

McGregor, G. R., and A. F. Gellatly, 1996: The energy balance of a melting snowpack in the French Pyrenees during warm anticyclonic conditions. *Int. J. Climatol.,* **16,** 1–8.

Moore, R. D., and I. F. Owens, 1984: Controls on advective snowmelt in a maritime alpine basin. *J. Climate Appl. Meteor.,* **23,** 135–142.

Ohmura, A., 1981: Climate and energy balance on arctic tundra, Axel Heilberg Island, Canadian Arctic Archipelago, Spring and Summer 1969, 1970 and 1972. Swiss Federal Institute of Technology, Zurich, Switzerland, 447 pp.

Petzold, D. E., 1981: The radiation balance of melting snow in open boreal forest. *Arct. Alp. Res.,* **13,** 287–293.

Pluss, C., and R. Mazzoni, 1994: The role of turbulent heat fluxes in the energy balance of high alpine snow cover. *Nord. Hydrol.,* **21,** 133–147.

Robinson, D. A., 1986: Initiation of spring snowmelt over Arctic lands. *Proc. Cold Regions Hydrology Symp.,* Fairbanks, AK, American Water Resources Association, 547–554.

——, 1989: Evaluation of the collection, archiving, and publication of daily snow data in the United States. *Phys. Geogr.,* **10,** 120–130.

Rowe, C. M., K. C. Kuivinen, and R. Jordan, 1995: Simulation of summer snowmelt on the Greenland ice sheet using a one-dimensional model. *J. Geophys. Res.,* **100,** 16 265–16 273.

Sheridan, S. C., 2002: The redevelopment of a weather-type classification scheme for North America. *Int. J. Climatol.,* **22,** 51–68.

Treidl, R. A., 1970: A case study of warm air advection over a melting snow surface. *Bound.-Layer Meteor.,* **1,** 155–168.

Yarnal, B., D. L. Johnson, B. J. Frakes, G. I. Bowles, and P. Pascale, 1997: The flood of '96 and its socioeconomic impacts in the Susquehanna River basin. *J. Amer. Water Resour. Assoc.,* **33,** 1299–1312.